# Transit Time Oscillations as a Source of EMC Problems in Bipolar Power Devices

Ralf Siemieniec
Technical University of Ilmenau
PO Box 100565
D - 98684 Ilmenau
Phone: +49 3677 693225
Fax: +49 3677 693777
e-mail: ralf.siemieniec@tu-ilmenau.de

Josef Lutz
Chemnitz University of Technology
D-09107 Chemnitz
Phone: +49 371 5313618
Fax: +49 371 5313327
e-mail: jlu@infotech.tu-chemnitz.de

Mario Netzel
Technical University of Ilmenau,
PO Box 100565
D - 98684 Ilmenau
Phone: +49 3677 693225
Fax: +49 3677 693777
e-mail: mario.netzel@tu-ilmenau.de

Paul Mourick
SEMIKRON Elektronik GmbH
Sigmundstraße 200
D - 90431 Nürnberg
Phone: +49 911 6559 219
Fax: +49 911 6559 77219
e-mail: paul.mourick@SEMIKRON.com

## Acknowledgements

The authors wish to thank the engineers from CE-SYS Electromagnetic Compatibility Testing Laboratory, especially Mr. Mario Tietze, for their support during the EMC measurements, and Dr. Hans-Peter Geromiller from the Chemnitz University of Technology for his comments concerning interpretation of the measurement results.
This work is supported by grants of the Deutsche Forschungsgemeinschaft.

## Keywords

Transit time oscillation, impact ionization, plasma extraction, high-frequency oscillation, electromagnetic compatibility

## Abstract

Transit time oscillations may occur in the turn-off phase of power devices and cause high-frequency oscillations. This paper investigates two mechanisms which lead to these oscillations: dynamic impact ionization transit time (IMPATT) oscillations and plasma extraction transit time (PETT) oscillations. Both lead to a deterioration of the EMC behavior and consequently they should be avoided.

## 1 Introduction

EMC issues are increasingly important today. EMC problems caused by LC oscillations, for instance as a result of a snap-off during the reverse recovery of freewheeling diodes, are commonly known. Solutions deal with an improvement of the device design and lead to a new generation of fast diodes avoiding a snap-off even under low current condition. Unlike these issues, the degradation of EMC properties due to high-frequency oscillations, as shown for example in figures 3 and 6, are less well-known. Nevertheless, due to the improvements in the design of devices as well as of converters, such effects come to the fore.
This work explains mechanisms which may cause the oscillations as well as basic possibilities for their prevention. EMC measurements give a clear evidence for the necessity for the prevention of these effects.

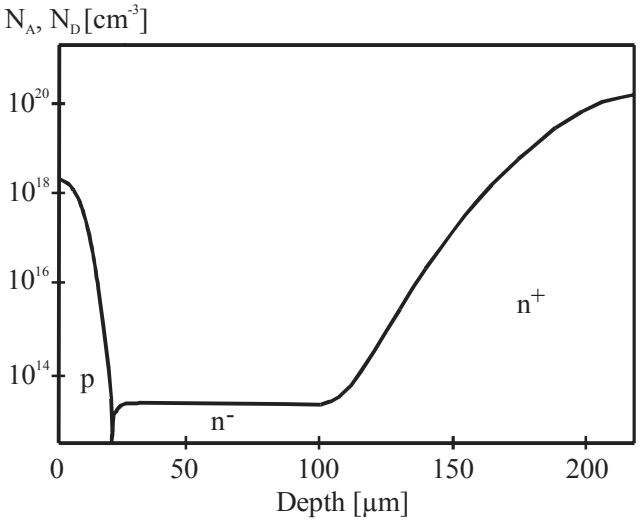


Figure 1: Basic structure of a 1.2kV freewheeling diode

# 2 Device Overview

## 2.1 Devices for Investigation of Dynamic IMPATT Oscillation

Different irradiated freewheeling diodes were compared with commercially available devices with identical voltage and current range. The doping profile of the devices is shown in figure 1.
Table I gives an overview about the different device types. All freewheeling diodes shown in table I are paired with an appropriate IGBT chip in a high side switch configuration [1].

## 2.2 Devices for Investigation of PETT Oscillation

For the investigations concerning PETT oscillations, experimental power modules, manufactured by SEMIKRON, were used. The ratings of both module types, GAR (high side switch) and GAL (low side switch), are given in table II. In these devices, two freewheeling diodes (FWD) as well as two IGBTs are either paralleled in one group at one DCB (direct copper bonding) substrate, while again two groups are paralleled in one module (see figure 13). Figure 2 shows the internal circuit of the two modules.
The doping profile of the FWDs inside the modules is identical to that already shown in figure 1.

**Table I: Devices used for EMC Measurements in case of IMPATT Oscillation**

| Device | Irradiation Type of FWD | Nominal Current | Nominal Voltage |
|---|---|---|---|
| SC45 | Electrons, E=4.5MeV, $d=1\cdot10^{15}\,cm^{-2}$ | 100A | 1200V |
| SKCD47C120I | SEMIKRON CAL-Diode | 100A | 1200V |
| SC14 | Helium ions, E=11.6MeV, $d=1.4\cdot10^{12}\,cm^{-2}$ | 9A | 1200V |
| SC21 | Helium ions, E=11.6MeV, $d=2.1\cdot10^{12}\,cm^{-2}$ | 9A | 1200V |
| SKCD11C120I | SEMIKRON CAL-Diode | 9A | 1200V |

**Table II: Devices used for EMC Measurements in case of PETT Oscillations**

| Device | Type | Nominal Current | Nominal Voltage |
|---|---|---|---|
| GAR | High side switch | 600A | 1200V |
| GAL | Low side switch | 600A | 1200V |

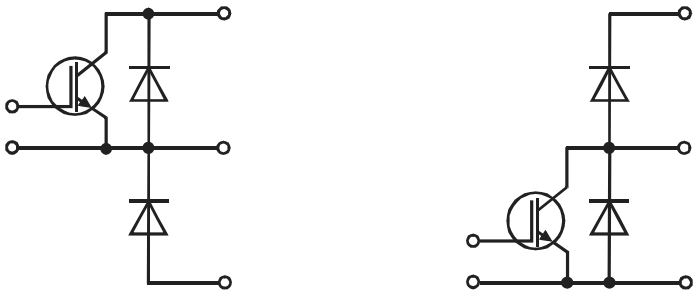

Figure 2: Internal circuit of the modules – high side switch GAR (left) and low side switch GAL (right)

# 3 Physical Mechanisms of Transit-Time Oscillations

## 3.1 Dynamic IMPATT Oscillation

IMPATT oscillations are known from Impatt- and other comparable transit-time diodes [2]. At a voltage above the stationary avalanche breakdown voltage, a high frequency signal is generated by these specially designed devices. In difference, dynamic IMPATT oscillations are caused by temporarily positively charged donor-states, which is one of the generated centers created by irradiation processes for carrier lifetime control. Irradiation processes allow the generation of homogenous carrier lifetime profiles using electron irradiation (beta particles) as well as local carrier lifetime profiles using hydrogen ions (protons) or helium ions (alpha particles). Figure 3 shows the measurement of a dynamic IMPATT oscillation at an electron-radiated freewheeling diode SC45. A short explanation of the effect is given on example of a common freewheeling diode structure with a basic doping profile as was shown in figure 1. Under forward bias, the generated donor-states are positively charged.

During the turn-off process, the generated donor-states remain positively charged and enhance the $n^-$-doping, which usually sustains the blocking voltage, and therefore reduce the reverse blocking capability. Avalanche breakdown occurs at the pn-junction region and generates electrons. These electrons counterbalance the positively charged donor-states and hence stop the avalanche generation of carriers. Due to the electric field, the electrons are transported to the $nn^+$-junction and again, avalanche generation starts at the pn-junction. The dynamic IMPATT oscillation stops as soon as the positive donors are discharged and the device is once more able to withstand the reverse voltage [3].

The onset voltage of IMPATT oscillations depends mainly on the concentration of the donor-like centers and on the temperature. While an analytical expression for the calculation of this threshold voltage was given earlier in [3], it is now possible to use 2D device simulation as shown first in [4].

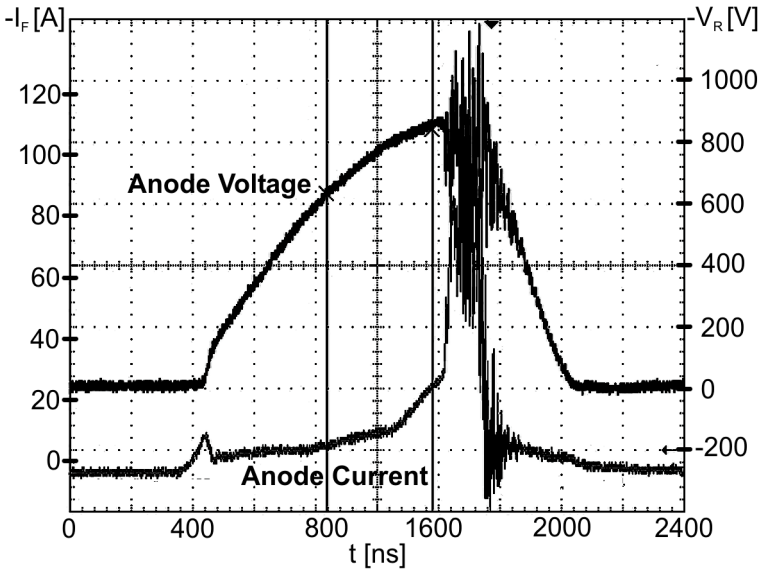


Figure 3: Measurement of a dynamic IMPATT oscillation at an electron-radiated freewheeling diode SC45 ($V_R$=910V, $I_F$=8A, di/dt=250A/µs, T=290K)

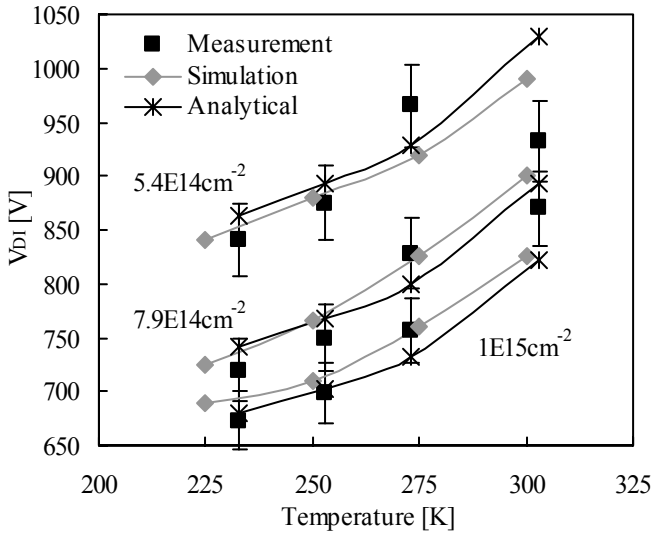


Figure 4: Trigger voltage of impatt oscillation for 4.5MeV electron-radiated devices in dependence of temperature and irradiation dose. Measured and analytical values taken from [3]

Figure 4 shows the comparison of measured, simulated and calculated values of the trigger voltage of IMPATT oscillations on example of electron-radiated recovery diodes.
IMPATT oscillation also occurs in helium-radiated, locally carrier lifetime controlled devices [5]. Figure 5 shows an example of the measurement of an IMPATT oscillation in a helium-radiated diode SC21 with a structure as shown in figure 1. Here, the peak of the recombination center profile was placed in a depth of app. 80µm. The voltage amplitude of the oscillation is much lower for this helium-radiated device compared to electron-radiated devices. The oscillation frequency, app. 1.4...1.6GHz in the measurement shown, is higher than the oscillation frequency of the electron-radiated sample. Due to the charged donor-states a temporary n-buffer is formed which results in a reduced width of the low-doped n-region. Moreover, the shape of the electric field becomes trapezoidal rather than the triangular characteristic of the electron-radiated device. This leads to a weaker temperature dependence of the trigger voltage of dynamic IMPATT oscillation in case of the helium-radiated devices [5].

### 3.2 PETT Oscillations

PETT oscillations are a recently discovered effect [6]. They were first observed in modules with

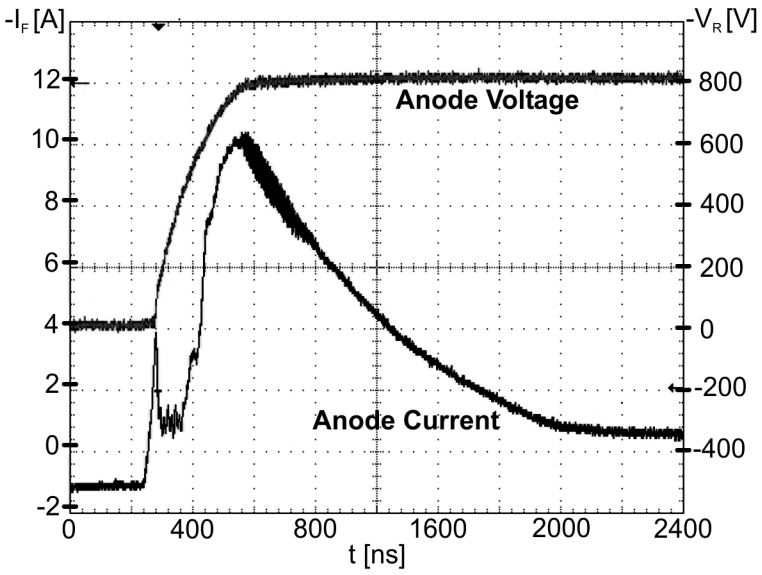


Figure 5: Measurement of a dynamic IMPATT oscillation at an helium-radiated diode structure SC21 ($V_R$=790V, $I_F$=1.5A, di/dt=250A/µs, T=275K)

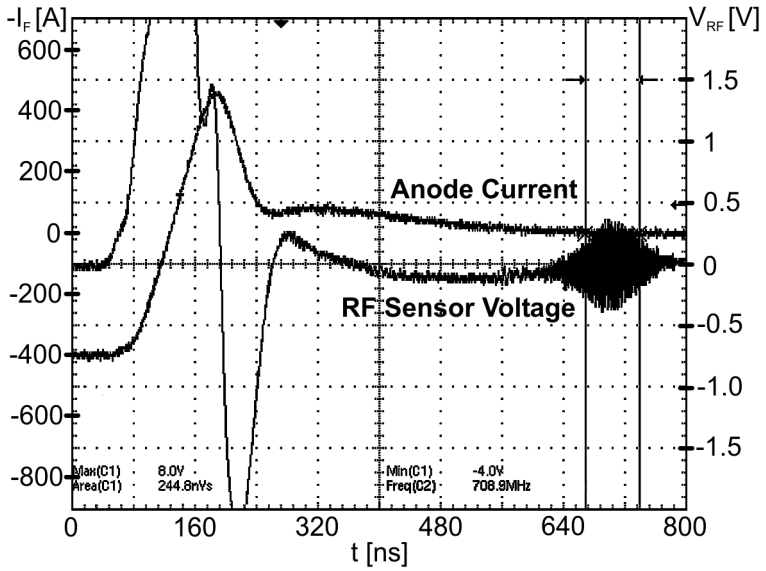


Figure 6: Measurement of a PETT oscillation in power module GAR with two paralleled diode chips ($V_R$=600V, $I_F$=200A, di/dt=4000A/µs, T=300K)

paralleled IGBT chips [6], but they were also found at paralleled freewheeling diodes and even in single IGBT chips [7]. Figure 6 shows the measurement of a PETT oscillation inside a power module with two paralleled freewheeling diodes. Here, PETT oscillation occurs while turning off the FWDs. The oscillation cannot be measured directly. Therefore an antenna was used to detect the electromagnetic field generated by the oscillations. The mechanism of this oscillation, which occurs in the tail phase of turn-off, is related to the oscillation mechanism of the BARITT diode [8]. In contrast to the BARITT effect, the carrier injection into the space charge region is caused by the stored excess carriers in the remaining plasma of the device during the turn-off process. Basically, the hole flow through the already formed space charge region has an almost constant velocity. This carrier transport results in a modulation of the electric field, therefore the change of the voltage across the device is delayed. Such a voltage delay causes a negative differential resistance. Oscillations occur if this negative differential resistance is larger than all other positive resistances in the complete circuit. In a simplified manner, the carriers travelling through the space charge region could be seen as a time-dependent displacement current (due to the removal of the stored excess carriers during turn-off). Oscillations appear as long as this displacement current coincides with critical values of the external inductance. Consequently, PETT oscillations occur only in interaction with a small external inductance. The onset of this oscillation further depends strongly on external parameters such as temperature (which considerably influences the value of the carrier drift velocity) or voltage. The device acts as the capacitive part of the resonance circuit. It should be explicitly mentioned, that the external inductance is mainly formed by the bond wires. Furthermore, the influence of the DCB (direct copper bonding) substrate capacitance is not negligible. Due to the high frequencies, which are governed by the power device structure, these oscillations are more likely to occur in modules realizing low parasitics.

# 4 General Estimation of EMC Problem Generation

In both cases (IMPATT and PETT), the oscillation frequency depends on the $n^-$-region width $w_B$ of the semiconductor device and the drift velocity $v_d$ of the carriers:

$$f \approx \frac{v_d}{w_B}$$

With a drift velocity of app. $10^7$cm/s, the frequency is in the range of 300...900MHz depending on the device thickness.

Dynamic IMPATT oscillations cause a high RF output power because a large number of carriers is generated which consequently lead to a strong modulation of the electric field. Not only do dynamic IMPATT oscillations result in a deterioration of the EMC parameters but they can also affect the drive

**Table III - Comparison of dynamic IMPATT and PETT Oscillation**

| Dynamic IMPATT Oscillation | PETT Oscillation |
|---|---|
| - estimated voltage amplitude: 200 - 400V | - estimated voltage amplitude: 20 - 30V |
| - large spurious radiation | - possibly leads to exceeding the EMC limits |
| - affects neighbored electronic components | - difficult to observe in measurements |
| - well-defined threshold voltage | - could arise by any voltage and/or temperature |
| - threshold voltage decreases with decreasing temperature | |
| - low influence of external LC-components | - needs a small external inductance |
| - positively charged donors temporarily reduce blocking voltage - avalanche breakdown | - carrier emission out of an region with high carrier density |
| - prevention by changed device design | - disappears by changing the external inductance, attenuation by eddy currents |

control units. According to [3], dynamic IMPATT oscillations can be safely avoided by proper device design if the parameters of helium- and electron irradiation are carefully chosen.
The output power of PETT oscillations is relatively low, but could result in exceeding the EMC limits. Preventing these oscillations is more difficult due to the high number of parameters which influence the resonance circuit. In general, the device, module and external circuit design should result in a mismatch of the internal and external resonance conditions. Known possibilities are the increase of the parasitic inductance between the individual chips by applying highly permeable materials [9] or by adding extra bond wires for direct connection of the chips [10].
Table III gives a short comparison between the characteristics of IMPATT and PETT oscillations.

# 5 EMC Measurements

## 5.1 Measurement Setup

The occurrence of high-frequency oscillations during the turn-off process of a power semiconductor results in an increase of electromagnetic emission. Consequently this could cause the emission limits to be exceeded by the device.
The EMC measurements presented in this work try to give an estimation of the emission caused by high-frequency oscillations in power semiconductors, holding evidence it is important to avoid or at least to minimize such effects. Of course, the exact noise level of a complete device is influenced by a large number of parameters. Here, only the problems arising from power semiconductors are investigated.

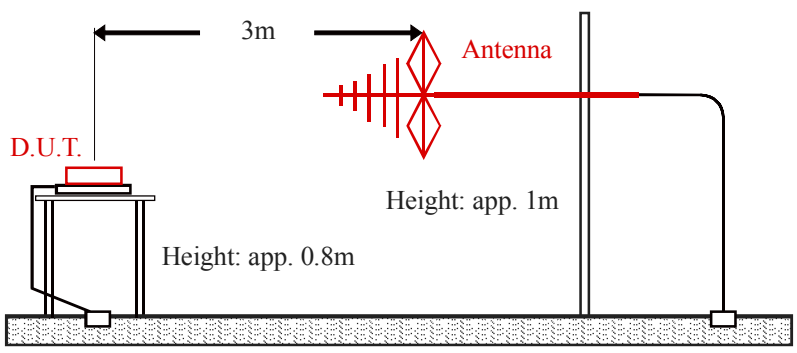


Figure 7: EMC measuring configuration

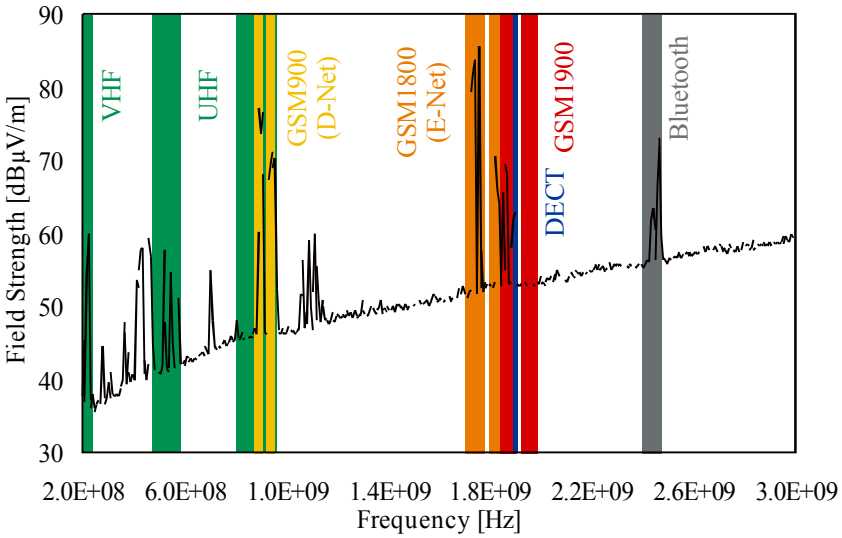


Figure 8: Measurement of environmental electromagnetic emission and frequency ranges of some typical emission sources (broadcast, telecommunications)

The permissible limit as well as the measuring method for ISM equipment (includes industrial, scientific and medical but excludes, for instance, telecommunication or information technology equipment, traction drives, equipment with electric drives etc. – in these cases, additional standards have to be taken into account) are defined by the European standard EN55011 (international standard IEC CISPR 11) [11]. This standard was taken into account for the EMC measurements, but according to the objective target of the measurements some changes were applied:

- The measurements were done in a usual, unshielded lab because of the high effort for transportation of the whole equipment needed for the transient characterization of fast–switching, high-voltage power devices. Therefore, the so-called environmental electromagnetic emission caused by typical emission sources such as mobile phones, broadcast, computers etc. has to be considered
- The distance between D.U.T. and antenna is reduced to 3m instead of 10m
- The measurements were taken in a frequency range of 200MHz-3GHz instead of 30MHz-1GHz

Figure 7 shows the basic configuration for the EMC measurements. For the measurements we used a logarithmic-periodical antenna manufactured by EMCO, Model 3147, and a Rohde&Schwarz spectrum analyzer, Model ESPI3.
Figure 8 shows the result of the environmental EMC measurement which covered a time span of two

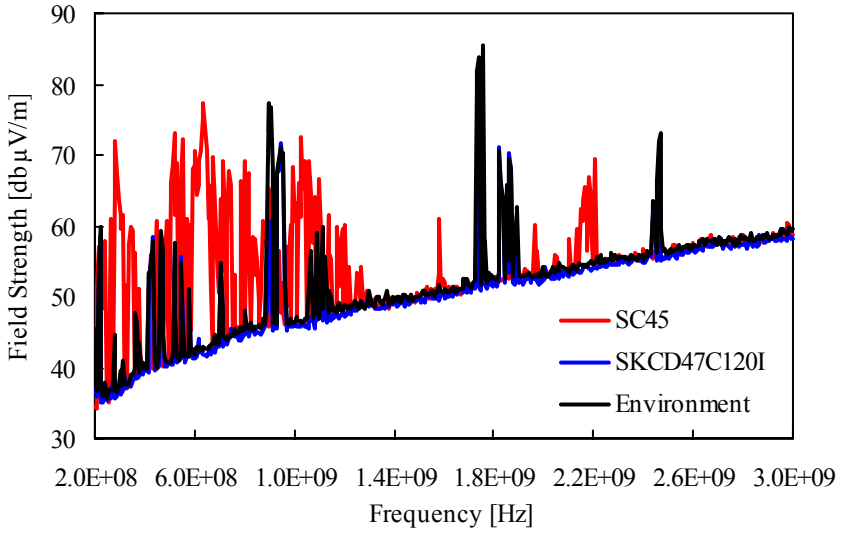


Figure 9: EMC measurement of SC45 (IMPATT) and SKCD47C120I in comparison with environment

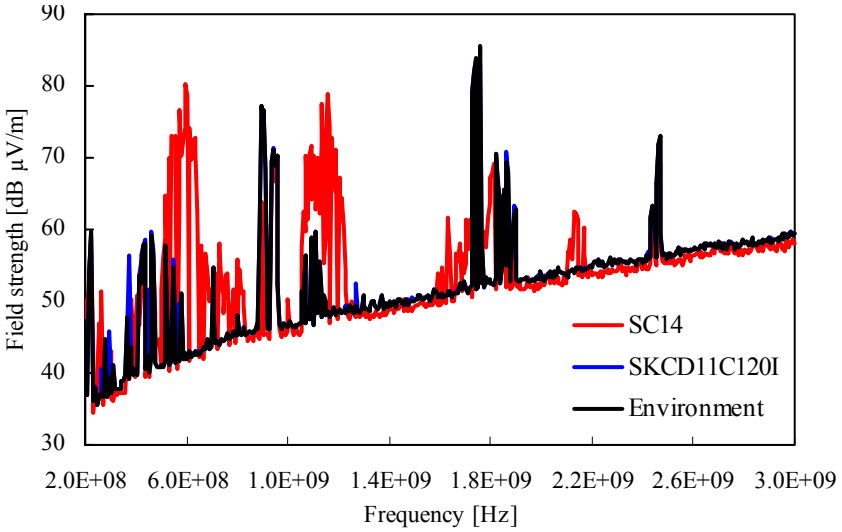


Figure 10: EMC measurement of SC14 (IMPATT) and SKCD11C120I in comparison with environment

hours, followed back-to-back by the subsequent measurements. The colored bars which are shown in figure 8 mark frequency ranges used by broadcast and telecommunication. Obviously, the largest interfering signals are caused by mobile communication equipment. This measurement series is included in all further figures to give evidence of additional generated signals which are caused by the transit-time oscillations.

## 5.2 Measurement Results for Dynamic IMPATT Oscillations

Figure 9 gives the comparison of the emission of SC45, exhibiting dynamic IMPATT oscillations, and of SKCD47C120I without any RF oscillations. The signals generated by SKCD47C120I are almost identical to the ones originating from the environment, whereas the IMPATT oscillations appearing while turning off SC45 (already shown in figure 3) cause a large increase in the emitted electromagnetic spectrum. Moreover, the emitted power leads to faults in the driver circuit. These malfunctions had to be prevented by additional shielding in order to enable these measurements. The maximum field strength was found at a frequency of app. 640MHz.
Figure 10 shows the comparison of the helium-radiated sample SC14 in comparison with the appropriate device SKCD11C120I. Here, the signals generated by dynamic IMPATT oscillation are less widespread and show a clear fundamental frequency of 600MHz as well as the first and second harmonic (although the second harmonic is superposed by environmental signals).
The emitted power is far less compared to SC45 and no problems were experienced even by using an

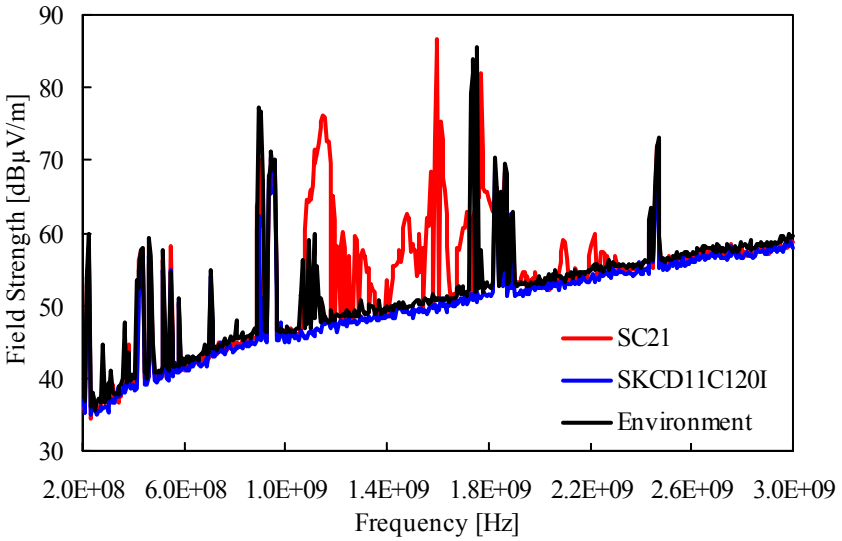


Figure 11: EMC measurement of SC21 (IMPATT) and SKCD11C120I in comparison with environment

unshielded driver circuit.
In case of the second helium-radiated device SC21, the results in terms of emitted power are quite similar. Nevertheless, the appropriate spectrum given in figure 11 shows some differences. Here, no fundamental oscillation in the frequency range of 600...650MHz is found. The maximum signal is detected at a frequency of 1.6GHz, while a second, less sharply bounded peak is found at app. 1.2GHz.
This different behavior is caused by the temporary n-buffer due to the charged donor-states (see chapter 3.1). In contrast to SC14, the density of the donor-states is significantly larger and results in a temporarily shortened $n^-$-region. Also, the time needed for discharging the donor-states is increased in case of SC21. Nevertheless, a part of these donor-states discharges over time, leading to an increase in the effective width of the $n^-$-region as well as of the transit-time of the carriers. As a result, the oscillation frequency decreases. The dynamic IMPATT oscillation of SC21 obviously stops before the temporary n-buffer is discharged due to the already reduced number of charged donor-states in the $n^-$-region. Therefore, no signal is found in the frequency range of the fundamental oscillation as it was present in SC45 and SC14.
All generated signals are sufficiently large to exceed the limits set by the EMC standards. For instance, the recommended field strength limit for ISM equipment in the frequency range above 1GHz is set to 70dB µV/m.

### 5.3 Measurement Results for PETT Oscillations

PETT oscillations were observed only in the high side switch GAR. The oscillations occur in the tail current as shown in figure 6. Figure 12 gives the comparison of EMC measurements of both module types as well as the environmental measurement. The PETT oscillation during the turn-off of GAR causes two sharp peaks in the frequency spectrum, appearing at 700MHz and 1.4Ghz, respectively, which could be assigned to the fundamental frequency and the first harmonic. The emitted power is relatively small compared to that found in case of dynamic IMPATT oscillations, but still app. 10dB larger than the signals found by turning off the low side switch GAL. Although the spurious radiation caused by PETT oscillation is lower, an exceeding of the EMC limits may nevertheless occur if more than one power module is used in the equipment which is expected to be the typical case.
In figure 13, the FWD reverse current flow through both of the modules is shown.
In comparison to module GAR, the current path through module GAL is substantially longer. Oscillations occur only in module type GAR. Although the resonance conditions are mainly set up by the displacement current of the FWD and the inductance of the bond wires, the capacitance of the particular DCB has a great effect, too. In case of module GAL, the total capacitance therefore differs from that of module GAR. Most likely, this leads to a mismatch of the resonance circuit and thus it explains, that no oscillations occured in this module.

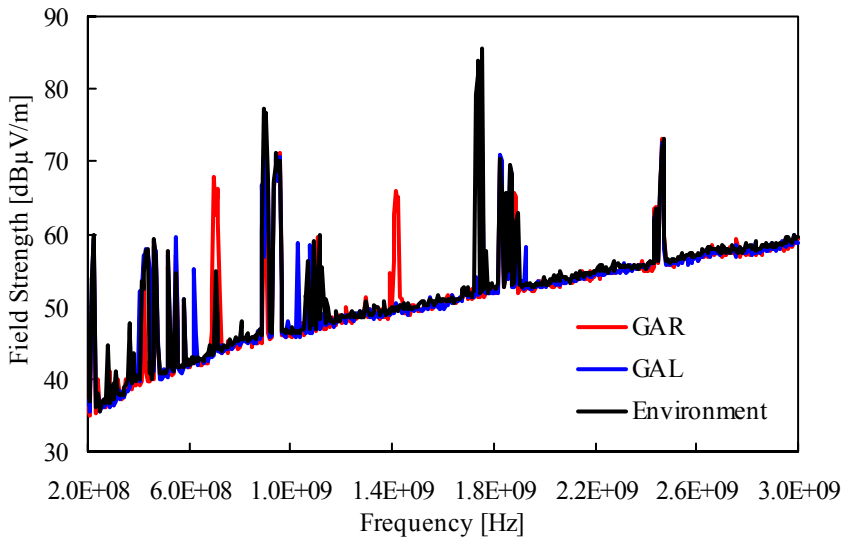


Figure 12: EMC measurement of GAR (PETT) and GAL in comparison with environment

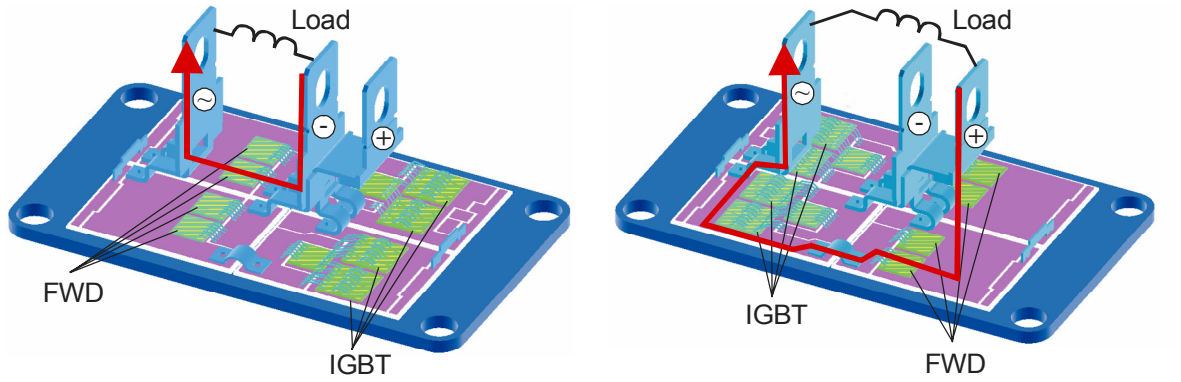


Figure 13: Module layout of GAR (left) and GAL (right) and current flow during turn-off process of the FWDs

## 6 Conclusion

High-frequency transit-time oscillations in bipolar power semiconductor devices may occur during the turn-off process. The oscillations investigated here are caused either by charged deep traps, generated by improperly controlled irradiation processes as used for carrier lifetime adjustment (dynamic IMPATT oscillations), or by carriers extracted from the excess carrier region remaining during the tail current phase due to interaction with parasitic inductances (PETT oscillations).
In this work, the possible influence of these undesirable oscillations on the electromagnetic emission is studied by using common EMC measurements. Although these measurements were performed under non-ideal lab conditions, the results show a strong increase of the total generated emission due to the RF oscillations. Moreover, the generated spurious radiation will increase further in typical applications, where usually more than one single chip is used. Therefore, it is recommended to avoid these oscillations since they may cause the EMC limits as defined by several standards to be exceeded.

## References

[1]. SEMIKRON International, Data Sheets

[2]. Sze, S.M.: Physics of Semiconductor Devices, 2nd Edition, John Wiley & Sons, New York, 1981

[3]. Lutz, J., Südkamp, W. and Gerlach, W.: Impatt Oscillations in Fast Recovery Diodes due to Temporarily Charged Radiation-Induced Deep Levels, Solid-State Electronics, 42 (6), 1998, 931-938

[4]. Siemieniec, R., Lutz, J.: Axial Lifetime Control by Radiation Induced Centers in Fast Recovery Diodes, Proc. ISPS 2002, Prague, 2002, 83-90

[5]. Siemieniec, R., Lutz, J., Herzer, R.: Analysis of Dynamic Impatt Oscillations caused by Radiation Induced Deep Centers", ISPSD 2003, Cambridge, 2003, 283-286

[6]. Gutsmann, B., Mourick, P., Silber, D.: Plasma Extraction Transit Time Oscillations in Bipolar Power Devices, Solid-State Electronics, 46 (5), 2002, 133-138

[7]. Mourick, P., Gutsmann, B., Silber, D.: Ultra High Frequency Oscillations in the Reverse Recovery Current of Fast Diodes, ISPSD 2002, Santa Fe 2002, 205-208

[8]. van de Roer, T.G.: D.C. and small-signal A.C. properties of silicon BARITT diodes, PhD Thesis, University of Eindhoven, 1977

[9]. Takahashi, Y., Koga, T., Yoshikawa, K., Yamazaki, K., Kirihata, H., Seki, Y., Eschrich, F.: 2.5kV/1.8kA Power Pack IGBT, ETG-Fachbericht 72, Bad Nauheim, 1998, 43-54

[10]. Zimmermann, W., Sommer, K.-H.: Patent DE 19549011C2, 1995

[11]. Deutsches Institut für Normung: DIN EN 55011 - Industrielle, wissenschaftliche und medizinische Hochfrequenzgeräte; Funkstörungen – Grenzwerte und Messverfahren, VDE-Verlag GmbH, Berlin, 2000